Numerical simulations of experiments on quasi-two-dimensional turbulence

B. Jüttner,[1,*] D. Marteau,[2] P. Tabeling,[2] and A. Thess[1]

[1]*Institute for Aerospace Engineering, Dresden University of Technology, 01062 Dresden, Germany*
[2]*Laboratoire de Physique Statistique, Ecole Normale Superieure, 24 rue Lhomond, 75005 Paris, France*

We report direct numerical simulations (DNS) of the two-dimensional (2D) Navier-Stokes equation, including a linear friction term which parallels a series of recent experiments on decaying quasi-2D turbulence in thin, stably stratified, fluid layers. If we start the DNS from the experimental situation when transient processes within the layers have died away, then quantitative comparison between simulation and experiment shows a remarkable agreement for the temporal evolution of the stream function and the vorticity field. The results confirm the two dimensionality of the experimental dynamics after a short initial period of relaxation and suggest the use of 2D simulations for extrapolating the observations to the case without bottom friction, inaccessible to experiments with stratified fluids. [S1063-651X(97)07804-5]

I. INTRODUCTION

The understanding of the dynamics of two-dimensional (2D) turbulence is a fundamental problem of theoretical fluid mechanics [1,2] with various applications to geophysics [3] and magnetohydrodynamics [4]. Although a lot of experimental and numerical work has been done to characterize particular properties of quasi-two-dimensional dynamics in rotating, stratified, or magnetohydrodynamic flows, there appears to be a lack of direct numerical simulations reproducing the transient dynamical evolution of experimentally determined vorticity fields starting from (almost) identical initial conditions. For instance, experiments on 2D turbulence in soap films could, to a certain degree, be reproduced by numerical simulations starting with idealized initial conditions [5]. However, the numerical vorticity field could not be quantitatively compared with the experimental one because the latter was not amenable to direct measurement. An impressive example of quantitative agreement between experiment and theory comes from the observation of equilibrium arrangements of 2D vortices, where measurements in superfluid helium [6,7] and in nondissipative pure electron plasma [8–12] show remarkable similarity with theoretical predictions. Nevertheless, in both cases the comparison involves static rather than dynamic states, in particular leaving open the question as to whether the dynamical evolution of quasi-2D electron plasmas is in quantitative agreement with direct simulations of the 2D Navier Stokes equation (NSE) or 2D Euler equation. A third example of successful intercomparison of 2D experiment and theory, involves aircraft measurements of one-dimensional energy spectra in atmospheric flows, which appear in good agreement with results of a closure model, including energy sources at small and large scales [13]. As in the preceding example, however, the comparison does not provide information about the power of 2D simulation in predicting the spatiotemporal evolution of specific vorticity fields. In summary, the question as to whether a 2D experiment and an appropriate 2D model, if started with identical initial conditions, would agree in the details of the vorticity field, remains open. The purpose of the present paper is to combine existing accurate vorticity measurements in 2D stratified fluids [14–16] with a 2D generalized NSE including linear friction [17–19] in order to perform a series of direct numerical simulations which parallel, to the greatest possible extent, the conditions of the reference experiment [15]. Even the investigation of the 2D model [17–19] and in particular, the influence of the linear friction term on the evolution of the quasi-2D flow becomes important for the determination of the range of validity and applicability of statistical theories of 2D turbulence. During the past decade three proposals for statistical descriptions of 2D turbulence have been made: The ''selective decay theory'' [20], the ''scaling theory'' [21], and the ''maximum entropy theory'' [22–24]. Each of them reports direct numerical simulations (DNS) which support their own theoretical predictions [25–29]. However, there is no investigation yet which is devoted to the question of whether the 2D equations of motion model experimentally realized quasi-2D flows. This question becomes particularly important in the light of recent experimental attempts [14–16] to test the statistical theories of 2D turbulence [20–24] which requires accurate tools.

The goal of the present communication is (i) a quantitative comparison of the spatial-temporal evolution in the experiment of Marteau, Cardoso, and Tabeling [15] (MCT), with a DNS of a 2D model [17–19] starting with data from the experimental initialization, (ii) the explanation of discrepancies between experiment and DNS by transient regimes of the vertical velocity profile in the first few seconds of evolution, and (iii) a detailed numerical study of the influence of the linear friction on the structure of the late states of the turbulent decaying vorticity fields.

Therefore, in Sec. II we will present a comparison between DNS and a special situation realized in the MCT experiment. Observed discrepancies shall be explained by relaxation processes within the fluid layers which cannot be modeled by a 2D equation of motion. However, it can be understood in the framework of a Stokes approximation for

---

*FAX: (49 351) 463-8087. Electronic address:
juettner@fz-rossendorf.de
www:http://www.tu-dresden.de/mwism/juettner/home.html

TABLE I. Physical and numerical parameters of the reported DNS: the linear friction coefficient μ, the viscosity exponent p ($p=1$: usual kinematic viscosity, $p=2$: hyperviscosity), the viscosity coefficient ν_p, the box size L, and the number of collocation points N.

Run no.	Initial condition	t_{start} [s]	t_{end} [s]	μ [s^{-1}]	p	ν_p [$m^{2p}s^{-1}$]	L [m]	N
1	disordered, expt. situation	0	20	0.07	1	8.3×10^{-7}	0.064	256^2
2	disordered, expt. situation	4	20	0.07	1	8.3×10^{-7}	0.064	256^2
3	disordered, expt. situation	0	20	0.07	1	1.0×10^{-8}	0.064	512^2
4	disordered, expt. situation	0	20	0.07	2	1.0×10^{-13}	0.064	256^2
5	disordered, expt. situation	0	120	0	1	6.0×10^{-8}	0.064	256^2
6	lattice, 4 altern. vortices	0	27	0.09	1	8.3×10^{-7}	0.064	256^2
7	lattice, 4 altern. vortices	0	35	0	1	2.8×10^{-7}	0.064	256^2
8	lattice, 16 altern. vortices	0	27	0.11	1	8.3×10^{-7}	0.096	256^2
9	lattice, 16 altern. vortices	0	189	0	1	1.2×10^{-7}	0.069	256^2

the initial phase of the MCT experiment which is done in Sec. III. In Sec. IV we will focus on the final organized states of 2D turbulence as obtained from DNS for several initial conditions, as used in the MCT experiment.

II. QUANTITATIVE COMPARISON OF DIRECT NUMERICAL SIMULATIONS WITH THE MCT EXPERIMENT

Recent experimental realizations of decaying quasi-2D turbulence have been performed using electromagnetic forces in order to establish initial distributions of quasiunidirectional vortices [14–16]. Quantitative measurements of the decaying 2D vorticity field and of the coefficient of linear friction have been done. Based on these experimental observations we perform DNS of the generalized 2D Navier-Stokes equation [17–19]

$$\frac{\partial \omega}{\partial t}+(\vec{v}\cdot\vec{\nabla}_2)\omega=(-1)^{p+1}\nu_p\Delta_2^p\omega-\mu\omega, \quad (1)$$

with

$$\omega(x,y,t)=[\vec{\nabla}_2\times\vec{v}(x,y,t)]\cdot\vec{e}_z \quad (2)$$

in a square domain $(x,y)\in D=[0,L]^2$. We suppose free slip boundary conditions at the lateral walls for the 2D velocity field $\vec{v}=v_x(x,y,t)\vec{e}_x+v_y(x,y,t)\vec{e}_y$ and vanishing vorticity ω at boundary ∂D. The 2D Nabla operator is denoted with $\vec{\nabla}_2=\vec{e}_x\partial/\partial x+\vec{e}_y\partial/\partial y$ and the 2D Laplacian with $\Delta_2=\vec{\nabla}_2^2$. The linear dissipative term models the bottom friction. The simulations use a modification of the pseudospectral code of Ref. [28] which is based on a vorticity-stream function representation of the model Eq. (1). Then the lateral boundary conditions are $\psi|_{\partial D}=\omega|_{\partial D}=0$, where the stream function is defined by $\vec{v}=\vec{\nabla}_2\times\psi\vec{e}_z$. We use spatial resolutions of $N=256^2$ or $N=512^2$ collocation points. The parameters of the DNS reported here are shown in Table I.

First we study the seemingly unusual case of a disordered system (runs nos. 1–5), because this initial condition does not possess any imposed symmetry and represents the generic case. For initialization of the simulation from an experimental situation or for comparison of the DNS with the experiment, we interpolate the experimentally measured vorticity fields from the original 40×40 grid up to the numerical resolution.

Run no. 1 is started from the experimental situation at $t=0$ when the electric current through the fluid layers has been turned off. For this simulation we suppose that within the three-dimensional (3D) fluid layers two dissipation mechanism act: a linear friction due to the vertical velocity profile and a usual 2D diffusion due to the horizontally acting parts of the 3D Laplacian. We choose $p=1$ in Eq. (1) and take the molecular viscosity as $\eta=10^{-3}$ k gm^{-1} s^{-1} (water). The fluid actually consists of two layers of salted water with densities $\rho_{1,2}=(1200\pm100)$ k gm^{-3}, which are approximated with a mean value of $\rho_0=1200$ k gm^{-3}. As result we get a kinematic viscosity $\nu_1=8.3\times10^{-7}$ m^2 s^{-1}. For the coefficient of the linear friction term we use the experimentally measured value $\mu=0.07$ s^{-1}. The initial minimum and maximum of vorticity are $\omega_{min,0}=-4.0$ s^{-1} and $\omega_{max,0}=3.3$ s^{-1}, respectively.

In Fig. 1 the evolutions of the vorticity fields in the experiment (center column), in the simulation run no. 1 (left column) and in the simulation run no. 2 (right column) are shown. The snapshots in the same row are taken at the same time. Now we compare the results of run no. 1 with the experimental observations. On the one hand, we observe a relatively good agreement when considering the large scale structures for each situation. More precisely, it is remarkable that the detailed merging events of nearby like-sign vortices are correctly reproduced by the numerical simulation [see e.g., the evolution of the (white) upper vortex triple at $t=0$ into a vortex pair at $t=4$ s]. On the other hand, discrepancies are visible in the shape and in the position of the large scale dipole at the late state ($t=20$ s) when most of the energy is dissipated due to the linear friction.

In the following we look at the temporal behavior of some integral quantities of the 2D flow. Let us consider the kinetic energy of the 2D velocity field

$$E=\frac{1}{2}\int_D \vec{v}^2 dD. \quad (3)$$
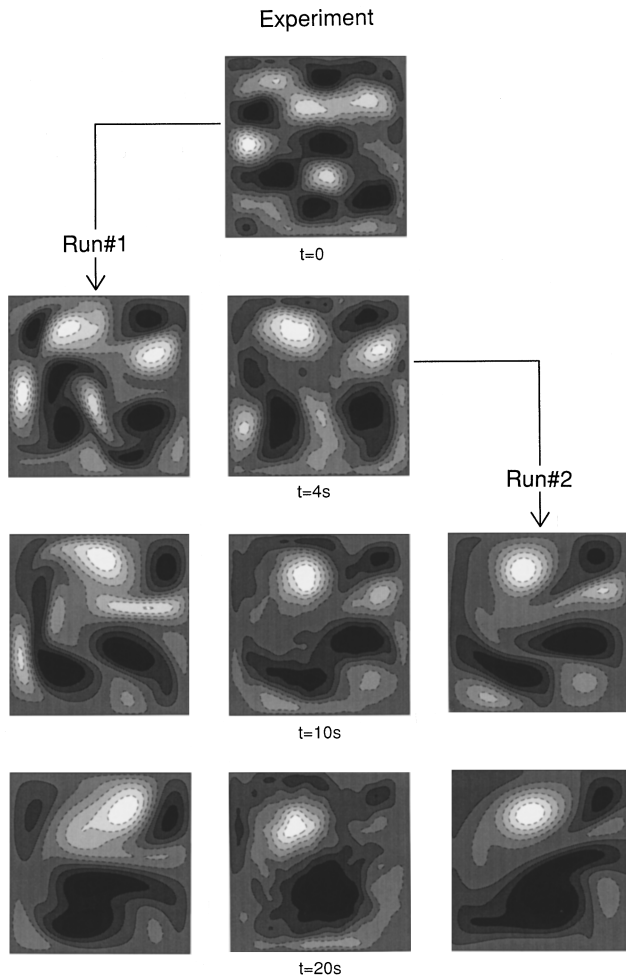
and the enstrophy of the vorticity

Experiment

FIG. 1. Evolution of the initially disordered vortex system in the MCT experiment [15] (center column) and in the DNS starting from the experimental situation at $t=0$ (run no. 1, left column) and starting from the initial experimental situation at $t=4$ s (run no. 2, right column). The linear friction and kinematic viscosity are taken as in the experiment. There are shown isovorticity plots at $t=0$, $t=4$ s, $t=10$ s, and $t=20$ s.

$$Z=\int_{D}\omega^{2}dD. \qquad (4)$$

In Figs. 2(a) and 2(b) the energy $\bar{E}=E/E_{0}$ and the enstrophy $\bar{Z}=Z/Z_{0}$ are shown as functions of time, respectively. Both quantities are normalized with respect to the values at $t=0$ which we denote with the index ''0.'' If we compare the results of run no. 1 (dotted lines) with the experimentally measured values (squares) we see that the energy and enstrophy in run no. 1 decay faster than in reality. These differences evolve in the first few seconds. In the experiment a slower decay of both $\bar{E}$ and $\bar{Z}$ is observed during the first few seconds than in the further evolution after $l\approx4$ s. Then, after $t\approx4$ s, the energy and the enstrophy of run no. 1 decrease with the same rate as in the experiment. However, the numerical values differ from the experimental values by an approximately constant factor of ≈0.5.

In spite of the latter discrepancies we have seen that the basic events of the evolution of the disordered system can be reproduced by model (1), starting at the experimental situa-
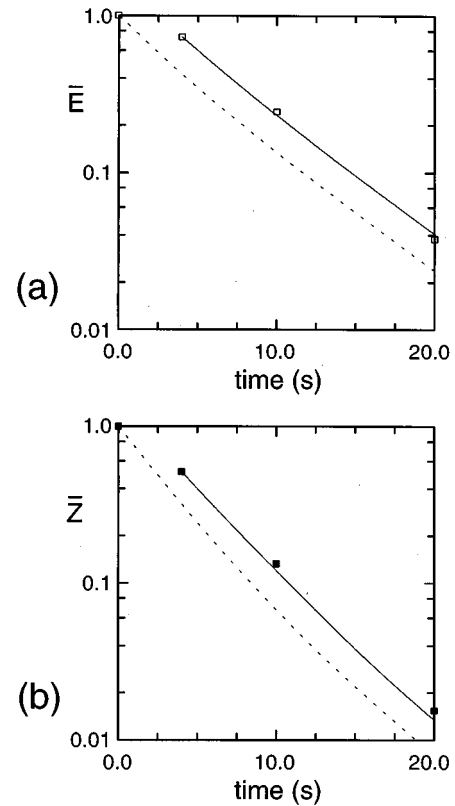

FIG. 2. Temporal behavior of the energy (a) and of the enstrophy (b) from the DNS starting at $t=0$ (dotted lines) and from the DNS starting at $t=4$ s (solid lines). The squares mark values which are measured in the MCT experiment [15]. The linear friction and kinematic viscosity are taken as in the experiment. The energy and the enstrophy are normalized with respect to their values at $t=0$.

tion at $t=0$. The duration of the initial period of discrepancies between numerical and experimental energy and entrophy decay, respectively, is of the order of the vertical viscous relaxation time of the leading higher order Stokes mode, $4h^{2}/9\pi^{2}\nu\approx1.93$ s with respect to experimental conditions. This suggests that 3D relaxation processes involving higher order Stokes modes may take place in the fluid, a conjecture that will be elaborated further in Sec. III.

Therefore, in run no. 2 we start the DNS from the experimental situation at $t=4$ s when most of the 3D relaxation processes should have disappeared. All the other conditions are the same as in run no. 1. Snapshots of the vorticity field from run no. 2 are shown in the right column of Fig. 1. Both at $t=10$ s and at $t=20$ s we observe an excellent agreement when comparing the size, the position, and the magnitude of the large scale vortices from the DNS with the experimentally observed arrangements (center column). In order to quantify the agreement between the simulations and the experiment we define a relative error

$$\delta(f)=\left(\frac{\int_{D}(f_{\mathrm{DNS}}-f_{\mathrm{EXP}})^{2}dD}{\int_{D}f_{\mathrm{EXP}}^{2}dD}\right)^{1/2}. \qquad (5)$$

We compute the relative error for the stream function $(f=\psi)$ and for the vorticity $(f=\omega)$ of run no. 1 and of run no.

TABLE II. Relative errors between the experimentally measured and the simulated stream function and vorticity fields for the disordered system: Comparison between DNS started at $t=0$ (run no. 1) and DNS started at $t=4$ s (run no. 2) both using experimental parameters.

t [s]	$\delta(\omega)$ [%]	$\delta(\psi)$ [%]	$\delta(\omega)$ [%]	$\delta(\omega)$ [%]
	run No. 1	run No. 2	run No. 1	run No. 2
0	0	-	0	-
4	42	0	68	0
10	55	16	92	45
20	60	31	92	61

2. The results are shown in Table II. We see that both the vorticity and the stream function fields of the simulation starting at $t=4$ s are in much better agreement with the experimentally measured data, than those of the simulation starting at the time $t=0$. In particular, we find a remarkably small error of only 16% for the stream function of run no. 2 at $t=10$ s when compared to the 55% of run no. 1. The large values of $\delta(\omega)$ should not be considered as a deficiency of the numerical simulation because they result from a comparison of the numerical fine grained vorticity field with the experimentally measured coarse grained vorticity. Again, considering the decay of energy and of enstrophy as shown in Figs. 2(a) and 2(b), respectively, we remark on the excellent agreement of the values from DNS run no. 2 (solid lines) with the experimentally measured values (squares). Therefore we can summarize that the simulation of the initially disordered arrangement of vortices shows reasonably good agreement in the frame of the spatial evolution and structure of the vorticity field, of the errors $\delta(\psi)$ and $\delta(\omega)$ and of the temporal behavior of $\bar{E}$ and $\bar{Z}$, when starting from the experimental situation at $t=4$ s.

Since the conservation of the scaled minimum and maximum vorticity

$$\bar{\omega}_{ext} = \frac{\omega_{ext}/\sqrt{E}}{\omega_{ext,0}/\sqrt{E_0}} \qquad (6)$$

was of particular experimental interest [14–16], we next turn to the temporal behavior of these quantities, which is shown in Figs. 3(a) and 3(b), respectively. The index ''ext'' stands for maximum or minimum. In the case of run no. 1 we observe a decay of both $\bar{\omega}_{min}$ and $\bar{\omega}_{max}$ down to 55% of the initial values at $t=20$ s. This observation is in disagreement with the experimental measurements for the disordered system. In the MCT experiment during the period from $t=4$ s up to $t=20$ s the scaled minimum was approximately conserved while the maximum was decaying further down to 68% of the initial value. While run no. 2 better reflects the integral quantities of the experiment than run no. 1, we do not observe a significant improvement with respect to the behavior of the global extrema shown in Fig. 3. Therefore we test the influence of the diffusion term of Eq. (1) on the conservation of the global extrema. We perform two DNS starting at $t=0$ and realizing higher Reynolds numbers than given in run no. 1 and run no. 2. At first we use in run no. 3 an usual kinematic viscosity which is 83 times smaller than
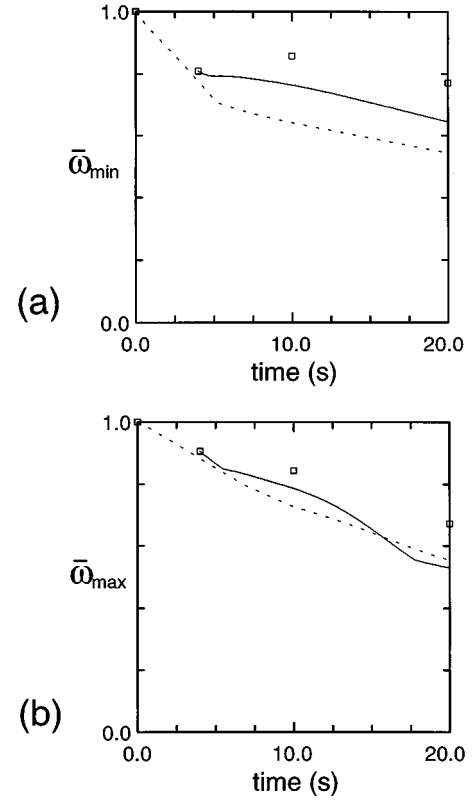

FIG. 3. Temporal behavior of the reduced global minimum of vorticity (a) and of the reduced global maximum of vorticity (b) from the DNS starting at $t=0$ (dotted lines) and from the DNS starting at $t=4$ s (solid lines). The squares mark values which are measured in the MCT experiment [15]. The linear friction and kinematic viscosity are taken as in the experiment. The global extrema of vorticity are normalized with respect to their values at $t=0$.

the kinematic viscosity in the experiment. In the second DNS, run no. 4, we choose hyperviscosity as the small scale dissipation mechanism. In both simulations we find a complete conservation of the global maximum of the vorticity. Considering the minimum of vorticity we observe a conservation of approximately 97% of the initial value when using hyperviscosity (run no. 4) but it decays down to 83% when applying an usual viscous term for diffusion of vorticity (run no. 3). Although these simulations show how to improve the agreement between DNS and the experiment with respect to the evolution of the global vorticity extrema, we find larger differences than in run no. 1 and in run no. 2 for the integral quantities and for the relative errors $\delta(\psi)$ and $\delta(\omega)$. The main difference between the experiment and the simulations with higher Reynolds number is visible when comparing the vorticity structures. We find that in run no. 3 and run no. 4 the diffusion does not act sufficiently in vortex merging processes. Then merging is not complete and small scale vortex filaments survive, which is not observed in the experiment.

We conclude, that higher Reynolds numbers generally improve the conservation of the global extrema of vorticity at the expense of a poor agreement in other observed features. As we have shown, the conservation of $\bar{\omega}_{ext}$ cannot be completely reproduced with our model Eq. (1), for the given initial data. We have identified two reasons for this, namely,

the lateral boundary conditions and 3D effects. The boundary conditions could play a role for the decay of $\overline{\omega}_{ext}$, if the global minimum or maximum come close to the box walls. Then the temporal behavior of this extremum should be influenced by the *different* boundary conditions in the experiment (no slip) and the DNS (free slip) at the lateral walls. We find that the global minima and maxima approach the boundaries up to distances of 5 mm and 9 mm, respectively, which could give rise to differences in the evolution of $\overline{\omega}_{ext}$ due to different boundary conditions. Furthermore, while model Eq. (1) describes the quasi-2D flow in a single layer fluid system the MCT experiment investigates the flow in a two layer system with a discontinuous stratification. However, in another experiment [14] without stratification of the thin fluid layer, two of the authors (Marteau and Tabeling) have observed a significant decay of $\overline{\omega}_{ext}$. Finally the influence of discontinous stratification within the two layer system on the temporal behavior of the global extrema of vorticity would require DNS of the complete 3D system including, also, the no slip boundary conditions on all walls, which is unfortunately much more expensive computationally.

Summarizing our results on the simulations of the disordered system and of the comparison with the results of the MCT experiment, we find that Eq. (1), including the experimental value of the viscosity and the experimentally measured decay rate of the linear friction, can be used as model for the quasi-2D flows, as studied in the MCT experiment. For quantitative comparison, the DNS should start after a short period of relaxation towards a Poiseuille profile within the fluid layers.

III. THE STOKES APPROXIMATION FOR THE INITIAL PERIOD

In this section we wish to propose a simple analytical model, based on the 3D linear Stokes equation that explains the reason for the postponement of energy and enstrophy decay in the MCT experiment (cf. Fig. 2). More precisely we will answer the following questions: What is the shape of the initial velocity profile across the 3D fluid layer at $t=0$? Is the velocity profile across the 3D fluid layer for times $t>0$ stationary or not? The answers to these questions are important in order to model the considered 3D system by the 2D equation (1) which contains the stationary linear friction term $-\mu\omega$ as the only remnat of the 3D origin. The reader interested only in the final results of the Stokes approximation should consult Fig. 5 where we show the decay of the square of vorticity at the surface for the dominating horizontal wave number. Indeed we find a postponement of this integral value, which is similar to the experimental behavior of the energy and entrophy decay, and is the result of the *nonstationary* velocity profile within the 3D fluid layer during the initial phase as we will show.

The model is based on the following physical ideas. Let us consider a 3D square box of horizontal dimension L which is filled with an electrically conducting fluid. The fluid layer has a thickness $h=0.006$ m and the upper surface is free and plane. An unidirectional electric current with a density $\vec{j}=j_0\vec{e}_x$ is conducted through the fluid. Furthermore, a magnetic field $\vec{B}=B_0\cos(\widetilde{m}x)\sin(\widetilde{n}y)\exp(-\gamma z)\vec{e}_z$, with

$\widetilde{m}=m\pi/L$ and $\widetilde{n}=n\pi/L$ is applied to the system (m and n are integers). The decay length of the magnetic field in vertical direction, $1/\gamma=0.003$ m, is known from measurements in the MCT experiment. At first we solve the stationary Stokes problem for the fluid which is driven due to the action of the chessboardlike Lorenz force $\vec{f}_L=\vec{j}\times\vec{B}$. In the second step we show that the experimentally measured horizontal velocity components are mainly caused by the z component of vorticity for which the initial vertical profile is calculated. In the third step we compute the decay of the square of the z component of vorticity at the upper surface when the electric current is turned off.

Applying the poloidal-toroidal decomposition [30] we find from the 3D Stokes equation

$$\frac{\partial\omega_z}{\partial t}=\nu\Delta\omega_z+A_1\sin(\widetilde{m}x)\sin(\widetilde{n}y)\exp(-\gamma z),\qquad(7)$$

for the z component of the 3D vorticity $\vec{\Omega}=\omega_x\vec{e}_x+\omega_y\vec{e}_y+\omega_z\vec{e}_z=\vec{\nabla}\times\vec{V}$ and

$$\Delta\frac{\partial v_z}{\partial t}=\nu\Delta^2 v_z+A_2\cos(\widetilde{m}x)\cos(\widetilde{n}y)\exp(-\gamma z),\qquad(8)$$

for the z component of the 3D velocity $\vec{V}=v_x\vec{e}_x+v_y\vec{e}_y+v_z\vec{e}_z$. We denote the 3D Nabla operator with $\vec{\nabla}=\vec{e}_x\partial/\partial x+\vec{e}_y\partial/\partial y+\vec{e}_z\partial/\partial z$. The 3D Laplacian is defined by $\Delta=\vec{\nabla}^2$. The inhomogeneous parts of Eqs. (7) and (8) have magnitudes $A_1=j_0B_0\widetilde{m}/\rho_0$ and $A_2=\gamma A_1\widetilde{m}/\widetilde{n}$. Although the experimental system [15] consists of two layers with densities $\rho_{1,2}=\rho_0(1\pm0.08)$, we suppose a homogeneous fluid with a density ρ_0, because the main part of the z dependence of the flow excitation results from the decaying magnetic field in a vertical direction. We consider now the stationary problem with $\partial/\partial t(.)\equiv0$ and insert $\omega_z=p_1(z)\sin(\widetilde{m}x)\sin(\widetilde{n}y)$ and $v_z=p_2(z)\cos(\widetilde{m}x)\cos(\widetilde{n}y)$ in Eqs. (7) and (8), respectively. We get

$$0=\nu(D^2-\beta^2)^i p_i-A_i\exp(-\gamma z)\quad(i=1,2)\qquad(9)$$

with $D=\partial/\partial z$ and $\beta^2=\widetilde{m}^2+\widetilde{n}^2$. Employing the boundary conditions [31]

$$p_1(0)=Dp_1(h)=p_2(0)=Dp_2(0)=p_2(h)=D^2p_2(h)=0\qquad(10)$$

we analytically solve the set of Eqs. (9). Using the definition of the vorticity, $\vec{\Omega}=\vec{\nabla}\times\vec{V}$, and the incompressibility condition, $\vec{\nabla}\cdot\vec{V}=0$, we get the velocity components

$$v_x=\frac{\pi^2}{L^2\beta^2}[\widetilde{n}p_1(z)-\widetilde{m}Dp_2(z)]\sin(\widetilde{m}x)\cos(\widetilde{n}y)\qquad(11)$$

and

$$v_y=\frac{\pi^2}{L^2\beta^2}[-\widetilde{m}p_1(z)+\widetilde{n}Dp_2(z)]\cos(\widetilde{m}x)\sin(\widetilde{n}y)\qquad(12)$$

in terms of the z components of $\vec{V}$ and $\vec{\Omega}$.

Now we can estimate the influence of the vertical component of the velocity, v_z, on the measurements of the horizontal velocity components which are used to reconstruct the 2D vorticity field of ω_z at the top of the fluid layer. We suppose for this estimation $\widetilde{m} = \widetilde{n}$ and evaluate the ratio $|Dp_2|/|p_1|$ at $z = h$ in dependence of the dimensionless wave number $\kappa = \beta h$ of the excitation. We find that the influence of v_z on the vertical velocity scales has a maximum at a certain wave number $\kappa_0 \approx 4$ and decreases for large wave numbers, which is shown in Fig. 4(a). In the experiment on the disordered system the energy is injected in a band of wave numbers. This band is limited by the minimum wave number, $\kappa_{min} \approx 0.41$, due to geometrical properties and by the maxi-

mum wave number, $\kappa_{max} \approx 24$, due to the dissipation length scale [2] $(\nu^2 L^2 / Z_0)^{1/4}$. We estimate the mean wave number of the energy injection in the case of the disordered system containing ten large scale vortices of the MCT experiment with $\kappa_E \approx 1.33$. Finally, we find that the horizontal velocity scales, i.e, v_x and v_y, are mainly connected with vertically directed vorticity lines $\omega_z \vec{e}_z$. This result justifies the use of Eq. (1) for $\omega \equiv \omega_z$ instead of both the fully nonlinear evolution equations [30,31] for ω_z and v_z. Therefore, if we neglect the influence of v_z on v_x and v_y, both the vertical vorticity component, and the horizontal velocity components depend on the same profile

$$p_1(\widetilde{z}) = \frac{A_1 h^2 \left\{ \exp(-\epsilon \widetilde{z})\cosh(\kappa) - \cosh[\kappa(1-\widetilde{z})] + \frac{\epsilon}{\kappa}\exp(-\epsilon)\sinh(\kappa\widetilde{z}) \right\}}{(\kappa^2 - \epsilon^2)\cosh(\kappa)} \tag{13}$$

with $\widetilde{z} = z/h$. In Fig. 4(b) profiles $p_1(z,\kappa)$ are shown for fixed parameter $\epsilon = \gamma h = 2$ as given from the MCT experiment. We see that for small wave numbers κ, i.e., for the large scales of forcing, a Poiseuille profile is established, and for intermediate values the profile becomes flat near the top of the fluid layer. However, the most surprising effect occurs for small scale excitations. Then we find an overshot in the profile, i.e., the maximum magnitude of horizontal motion is located near the bottom and the profile decays towards the free surface. Moreover, the overshots of the profile $p_1(z)$ are only caused by the decay of the magnetic field across the 3D fluid layer. If the magnetic field is constant within the 3D layer ($\epsilon \rightarrow 0$), then $p_1(z)$ is a monotoneously increasing function of and there does not exist overshots.

We next show that the shape of the profile $p_1(z)$ for $\kappa = \kappa_E$, which consists of a sum of vertical eigenmodes, causes a slower decay of the 2D motion at the top of the layer during the first few seconds in the MCT experiments than predicted when supposing purely linear friction. Let us consider the case when the flow has fully relaxed to the stationary profile $p_1(z, \kappa_E)$. Then the electric current is turned off. The flow decays. The decay depends both on the planar and the vertical action of the 3D Laplacian. We insert $\omega_z = \sum_{i=0}^{\infty} r_i(z,t)\sin(\widetilde{m}x)\sin(\widetilde{n}y)$, with $\sum_{i=0}^{\infty} r_i(z,t=0) = p_1(z,\kappa_E)$ in Eq. (7), while we have to set $A_1 = 0$ in order to model the free decay of ω_z at the surface. Solving the resulting eigenvalue problem we find $r_i = a_i \sin(\chi_i \pi z / h)\exp\{-(\nu/h^2)[(\chi_i \pi)^2 + \kappa_E^2]t\}$, with $\chi_i = i + 1/2$ and $a_i = \sqrt{2}\int_0^h p_1(z,\kappa_E)\sin(\chi_i \pi z/h)dz$. Since we are interested in the decay of the 2D flow at the surface, we consider the surface vorticity

$$w_s = \sum_{i=0}^{\infty} r_i(z = h, t)$$

$$= \sqrt{2}\sum_{i=0}^{\infty} a_i(-1)^i \exp\left\{ -[(\chi_i \pi)^2 + \kappa_E^2]\frac{\nu t}{h^2} \right\}. \tag{14}$$

There are two mechanisms of dissipation due to the 3D Laplacian: the decay proportional to $\exp[-(\kappa_E^2 \nu/h^2)t]$ belongs to the 2D Laplacian Δ_2 and does not depend on i, while $\sum_{i=0}^{\infty} a_i(-1)^i \exp[-(\pi^2 \nu/h^2)(i+1/2)^2 t]$ reflects the decay due to the friction in the vertical direction. We see that if the initial profile p_1 has only one nonvanishing coefficient a_0, then the decay due to the friction in the vertical direction is proportional to $\exp[-(\pi^2 \nu/4h^2)t]$, for all times $t \geq 0$, and it is possible to model this friction with a linear term which has a constant coefficient, $\mu = \nu\pi^2/4h^2$. Otherwise, if the initial profile p_1 consists of a sum of several nonvanishing parts, then these terms can compensate each other for a certain time period and the decay, due to the vertical friction, cannot be modeled by a single term $\exp(-\mu t)$ for all times. However, the higher order terms decay very fast for large values of i. Therefore, after a time period, which is of the order of the characteristic damping time of the leading higher order Stokes mode, $\tau_1 \approx 1.93$ s for $i = 1$, the only surviving term is $a_0 \exp[-(\nu\pi^2/4h^2)]$. Starting an observation at this instant, the decay of the 2D flow at the surface due to the friction in the vertical direction can be modeled by a single linear term, for instance $-\mu\omega$, as used in Eq. (1). In order to test these arguments we compute $\bar{\omega}_s^2 = \omega_s^2/\omega_{s,0}^2$, which is an integral measure of the quasi-2D flow at the surface comparable to the kinetic energy (3) or the entropy (4). Looking at Fig. 5 we find that during the first few seconds the decay of $\bar{\omega}_s^2$ is weaker than for larger times. After approximately 5 s the decay is proportional to $\exp(-\mu t)$. Comparing the evolution of $\bar{\omega}_s^2$ with the experimentally measured energy (empty squares) and enstrophy (solid squares) we see that the energy decays slower and the enstrophy decays faster than predicted by the Stokes approximation. This behavior can be explained by the nonlinear shift of the energy towards larger scales and entropy towards smaller scales, where small scales are dissipated faster than larger 2D scales. But, nevertheless, we see that for $t \geq 4$ s both the energy and the entropy decay exponentially with constant rate. Recent measurements of the velocity field, in the upper and the lower layer have been
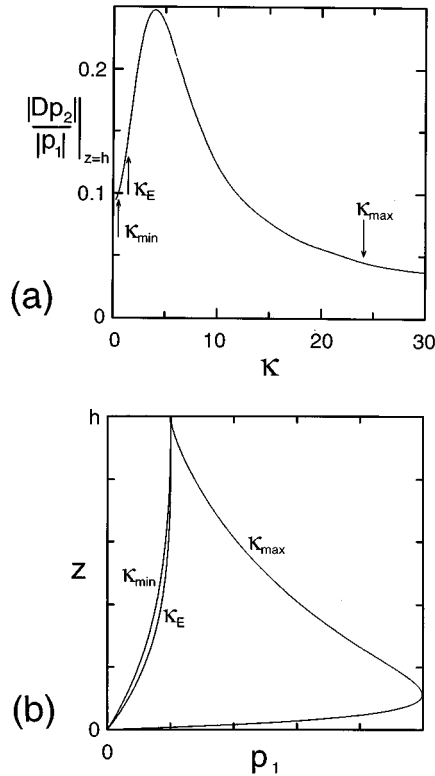
FIG. 5. Temporal behavior of the square of the velocity profile at the surface w_s^2, for the wave number of the energy containing structures κ_E (solid line). The dashed line marks the asymptotic behavior of w_s^2. For comparison the energy (empty squares) and the entrophy (filled squares) as measured in the MCT experiment [15] and normalized with respect to their values at $t=0$ are plotted.

FIG. 4. Analytic solution of the stationary 3D Stokes problem for a single fluid layer in a box with free surface at the top and an applied chessboardlike forcing of exponentially decaying strength in vertical direction: Ratio of the spatial change of the vertical velocity component, Dv_z, to the z component of the vorticity ω_z at the top of the fluid layer in dependence of the forcing wave number κ (a); profiles of the z component of the vorticity, ω_z, within the fluid layer (b). κ denotes the forcing wave number. κ_{min} is the minimal possible value with respect to the geometry. κ_E is the wave number of the energy containing structures, and κ_{max} is the wave number of the Kolmogorov dissipation scale.

do not find a monotonic function for the scatter plots in Figs. 6(a) and 6(b), indicating that, at this time, the system is not fully relaxed to an equilibrium state. We find this observation in agreement with the experiment, where only a partial

carried out, for the stratified system, in a situation where initially, kinetic energy is injected in the lower layer (no forcing takes place in the upper one). These measurements [32] have shown that it takes roughly two seconds to transfer energy across the entire fluid layer. After this transient state, velocities at the fluid interface between the two layers and at the free surface are found to have comparable amplitudes and decay at the same rate.

IV. THE FINAL STATES

Now we turn to the question of whether the experimentally observed final states of 2D turbulence for several initial conditions, i.e., both for disordered and for chessboardlike arrangements of alternating vortices, are equilibrium states of 2D turbulence or not. The maximum entropy theory [22–24] predicts monotonic $\psi-\omega$ relations for equilibrium states of 2D turbulence. In order to check this for the disordered system, we are looking at the $\psi-\omega$ scatter plot of the late state which we obtain as result of the simulation starting at $t=0$ [run no. 1, Fig. 6(a)] or starting at $t=4$ s [run no. 2, Fig. 6(b)]. Although the left tail of the scatter plot in Fig. 6(b) seems to be better relaxed towards a unique dependence, we
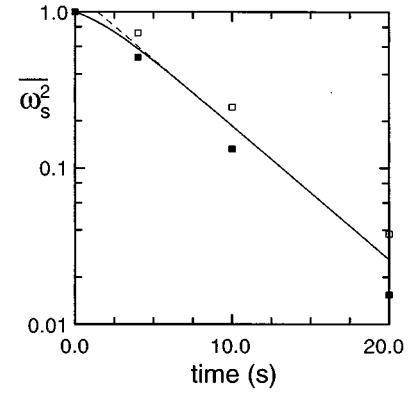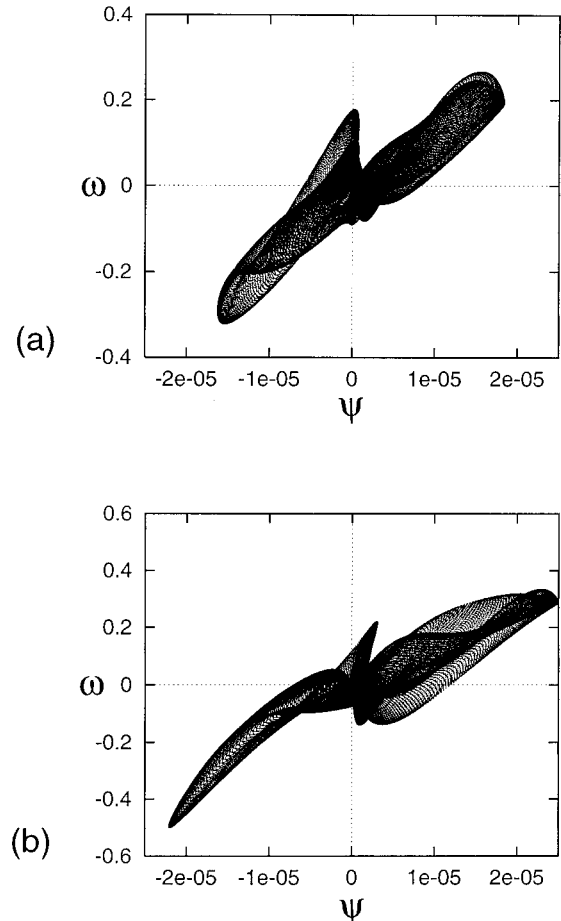

FIG. 6. $\psi-\omega$-scatter plot of the late state in the DNS at $t=20$ s for the initially disordered system of the MCT experiment [15] starting from the situation at $t=0$ (a) and at $t=4$ s (b).
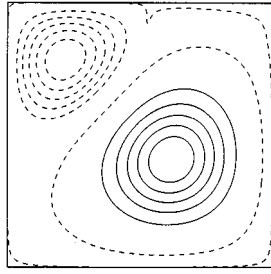
FIG. 7. Isovorticity plot of the late state ($t=120$ s) in the DNS starting from the initially disordered vortex system, without linear friction and an initial Reynolds number Re$=14\times$Re$_{exp}\approx3300$.

relaxation towards equilibrium has been noted [15]. However, what will happen if we remove the linear friction term, corresponding to a hypothetic experiment with zero bottom friction? In order to study the long term evolution of the flow, in the next step, the linear friction is removed from our model and the Reynolds number is increased to Re$=14\times$Re$_{exp}\approx3300$ which is as high as possible for the given spatial resolution of the DNS (cf. run no. 5 in Table I). Looking at the late state, for $l=120$ s, we find that the system relaxes into a diagonal dipole (Fig. 7). At this time approximately 62% of the initial energies are still concentrated in this large scale structure. Considering the $\psi-\omega$ relation (Fig. 8), we can see that this state is actually very close to a steady state. Notice that there is a symmetry breaking between positive and negative vorticity (cf. [29]).

Next, we turn to the other experimental realizations [15], possessing a high degree of symmetry. More precisely, the initial condition in MCT consisted of chessboardlike arrangements of $N=4$ and $N=16$ alternating vortices, respectively, which we model by sinuously shaped distributions $\omega(x,y,t=-t_i)=(1+\xi)\sin(2\pi kx/L)(2\pi ky/L)$. They comprise $N=4k^2$ counter-rotating vortices on which an additional random perturbation ξ with an amplitude of 1% is imposed. In the DNS, the initial vortex arrays become unstable after a time scale t_i which we take as the starting point ($t=0$) of the simulations on the decaying 2D turbulence. At this moment we scale the vortex field to magnitudes ω_N as measured in the experiments ($\omega_4=8.5$ s^{-1}, $\omega_{16}=7.4$ s^{-1}; for the parameters cf. runs nos. 6–9 in Table I).
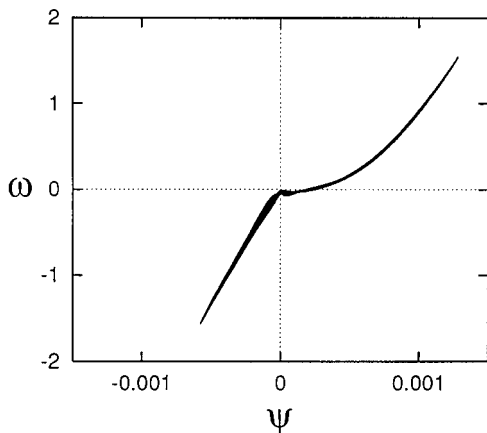

FIG. 8. $\psi-\omega$-scatter plot at $t=120$ s in the DNS of the initially disordered vortex system, using $\mu=0$ and Re$=14\times$Re$_{exp}\approx3300$.
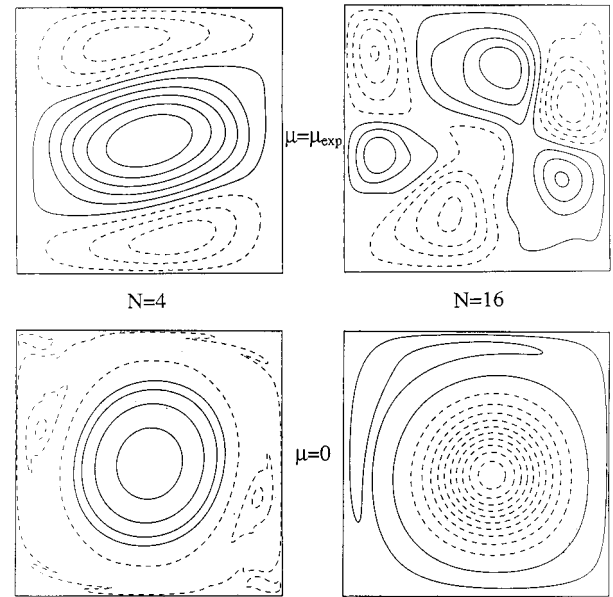

FIG. 9. Late states in DNS including the linear friction coefficient and the kinematic viscosity as taken in the experiment (upper row) and without of linear friction (lower row) starting from the 4-vortex system (left column) and from the 16-vortex system (right column): Isovorticity plots at $t=27$ s (upper row), at $t=35$ s (lower left, Re$=3\times$Re$_{exp}\approx3300$) and at $t=189$ s (lower right, Re$=7\times$Re$_{exp}\approx3300$).

First we consider the simulations including the linear friction (run no. 6 and run no. 8). We are looking at the states close to the final observation times of the experiments that is at $t=27$ s. Starting the evolution with four alternating vortices, we finally find a structure closed to a monopole (upper left plot in Fig. 9) in relative agreement with the MCT Fig. 1(d). In the experiment, however, the monopole is more akin to an annular structure, as in the DNS. Two effects can be responsible for this discrepancy: (i) the different boundary conditions at the lateral walls (no slip in the experiment and free slip in the DNS), in particular, act at the outer edge of the monopole and (ii) if the coefficient of the linear friction is overestimated from the experiment, then the effective time of evolution is too short for establishing the fully annular structure (cf. the arguments below). For 16 initial vortices we find a multipole as final state (upper right plot in Fig. 9), which has also been observed in the experiment [16]. However, by removing the linear friction term from Eq. (1) the picture changes. We take the Reynolds numbers as high as possible for the given spatial resolution (Re$=3\times$Re$_{exp}$ for the 4-vortex system and Re$=7\times$Re$_{exp}$ for the 16-vortex system; for the parameters cf. run no. 7 and run no. 9 in Table I) in these simulations. Then we find both for $N=4$ at a time $t_4=12$ s and for $N=16$ at a time $t_{16}=149$ a *transition* to a monopole. The finally observed states are fairly relaxed into annular structures at $t=35$ s in the case of the 4-vortex system (lower left plot in Fig. 9) and at $t=189$ s in the case of the 16-vortex system (lower right plot in Fig. 9). Concerning applications of the maximum entropy theory [22–24] in the case of a box geometry [29], we find the organization into a monopole, both for the case $N=4$ and for the case $N=16$, in agreement with the predictions of this theory.

Considering the results from the model Eq. (1) in com-

parison to simulations without of linear friction we have found differences with respect to the organization of the late states. We interpret these results as follows: On the one hand, for moderately high Reynolds numbers, as in our system, the linear friction is the main mechanism causing dissipation. Then a transformation

$$\widetilde{\omega} = \omega \, \exp(\mu t), \tag{15}$$

$$\widetilde{t} = \frac{1 - \exp(-\mu t)}{\mu} \tag{16}$$

formally leads to the Euler equation [32]

$$\frac{\partial \widetilde{\omega}}{\partial \widetilde{t}} + (\widetilde{\vec{v}} \vec{\nabla}) \widetilde{\omega} = 0 \tag{17}$$

with $\widetilde{\omega}(x,y,\widetilde{t}) = [\vec{\nabla} \times \widetilde{\vec{v}}(x,y,\widetilde{t})] \vec{e}_z$. However, the transformed time $\widetilde{t}$ is bounded by

$$\widetilde{t}_{max} = \lim_{t \to \infty} \widetilde{t}(t) = \frac{1}{\mu} \tag{18}$$

in contrast to the original Euler equation where the time is unlimited. In the original system this fact appears as a limitation of the particle path length which is restricted by

$$s_{max} \leqslant \frac{L\omega_0}{\mu}, \tag{19}$$

where ω_0 is the initial magnitude of vorticity. On the other hand, it has been shown that the necessary time of the organization of the equilibrium increases with the number of initial vortices. In particular, in the simulations starting from chessboardlike arrangements of alternating vortices, it has been shown for the 4-vortex system that the symmetry breaking occurs at a time t_4 which is approximately of the same order as $1/\mu_4$, otherwise, in the case $N=16$, the transition towards a monopole takes place at a time $t_{16} \gg 1/\mu_{16}$. Therefore, when comparing the late states of the simulations with and without linear damping, we can conclude that for a certain class of initial conditions (typically ordered lattices with many vortices, such as the 16-vortex system) complete relax-

ation towards the equilibrium is not reached, because the characteristic damping time is smaller than the time necessary for the large scale organization. The fact that the organization time is substantially smaller for the disordered 10-vortex state makes the observation of the final state possible in this particular case, using the same experimental system. This suggests that other parameters, such as the initial symmetry of the spatial vorticity distribution, have an influence on the way of relaxation which is taken by the system.

V. CONCLUSION

We summarize the main results of the present communication as follows: (i) Decaying quasi-2D turbulence in thin layers of stably stratified flows which are initially excited by electromagnetic forces can be simulated using Eq. (1). In particular, if starting a simulation at a time when the velocity profile within the fluid layers has relaxed to a Poiseuille profile, then this model of 2D turbulent flows corresponds, to a large extent, to the MCT experimental situations. (ii) Most of the discrepancies between the MCT experiment and the DNS of the 2D model Eq. (1) result from the nonstationary behavior of the velocity profile within the 3D layer which cannot be modeled by single linear term in a 2D equation. Considering the MCT experimental situation the vertical decay of the magnetic field excites higher order Stokes modes which exponentially decay with different rates and, therefore, cause the nonstationarity of the velocity profile. (iii) The finite mixing time of the system with bottom friction affects the structure of the experimentally observed late states when starting with a large number ($N \geqslant 16$) of initial vortices. (iv) The problem of the conservation of the global extremum of vorticity in a stratified system is still an open question which cannot be answered by a purely 2D approach. It is important because it is linked to the issue of how to model geophysical situations where stratification occurs.

[1] R. H. Kraichnan and D. Montgomery, Rep. Prog. Phys. **43**, 547 (1980).

[2] U. Frisch, *Turbulence* (Cambridge University Press, Cambridge, England, 1995).

[3] J. Pedlosky, *Geophysical Fluid Dynamics* (Springer-Verlag, New York, 1987).

[4] J. Sommeria and R. Moreau, J. Fluid Mech. **118**, 507 (1982).

[5] Y. Couder and C. Basdevant, J. Fluid Mech. **173**, 225 (1986).

[6] L. J. Campbell and R. M. Ziff, Phys. Rev. B **20**, 1886 (1979).

[7] E. J. Yarmchuk, M. J. V. Gordon, and R. E. Packard, Phys. Rev. Lett. **43**, 214 (1979).

[8] T. B. Mitchell, C. F. Driscoll, and K. S. Fine, Phys. Rev. Lett. **71**, 1371 (1993).

[9] X.-P. Huang and C. F. Driscoll, Phys. Rev. Lett. **72**, 2187 (1994).

[10] T. B. Mitchell and C. F. Driscoll, Phys. Rev. Lett. **73**, 2196 (1994).

[11] X.-P. Huang, K. S. Fine, and C. F. Driscoll, Phys. Rev. Lett. **74**, 4424 (1995).

[12] K. S. Fine, A. C. Cass, W. G. Flynn, and C. F. Driscoll, Phys. Rev. Lett. **75**, 3277 (1995).

[13] D. K. Lilly, J. Atmos. Sci. **46**, 2026 (1989).

[14] O. Cardoso, D. Marteau, and P. Tabeling, Phys. Rev. E **49**, 454 (1994).

[15] D. Marteau, O. Cardoso, and P. Tabeling, Phys. Rev. E **51**, 5124 (1995).

[16] D. Marteau and P. Tabeling (unpublished).

[17] J. C. McWilliams, J. Fluid Mech. **146**, 21 (1984).

[18] M. E. Maltrud and G. K. Vallis, J. Fluid Mech. **228**, 321 (1991).

[19] S. D. Danilov, F. V. Dolzhanskii and V. A. Krymov, Chaos **4**, 299 (1994).

[20] W. H. Matthaeus, W. T. Stribling, D. Martinez, S. Oughton, and D. Montgomery, Phys. Rev. Lett. **66**, 2731 (1991).

[21] G. F. Carnevale, J. C. McWilliams, Y. Pomeau, J. B. Weiss, and W. R. Young, Phys. Fluids A **4**, 1314 (1992).

[22] G. A. Kuzmin, in *Structural Turbulence*, edited by M. A. Goldshtik (Novosibirsk, City, 1982), p. 103.

[23] J. Miller, Phys. Rev. Lett. **65**, 2137 (1990).

[24] R. Robert and J. Sommeria, J. Fluid Mech. **229**, 291 (1991).

[25] W. H. Matthaeus, W. T. Stribling, D. Martinez, S. Oughton,

and D. Montgomery, Physica D **51**, 531 (1991).

[26] J. B. Weiss and J. C. McWilliams, Phys. Fluids A **5**, 608 (1993).

[27] J. Sommeria, C. Staquet, and R. Robert, J. Fluid Mech. **233**, 661 (1991).

[28] A. Thess, J. Sommeria and B. Jüttner, Phys. Fluids **6**, 2417 (1994).

[29] B. Jüttner, A. Thess, and J. Sommeria, Phys. Fluids **7**, 2108 (1995).

[30] O. Thual, J. Fluid Mech. **240**, 229 (1992).

[31] S. Chandrasekhar, *Hydrodynamic and Hydromagnetic Stability* (Oxford University Press, New York 1961).

[32] J. Paret, O. Paireau, D. Marteau, and P. Tabeling (unpublished).